State-Resolved Reactivity of $CH_4(2\nu_3)$ on Pt(111) and Ni(111): Effects of Barrier Height and Transition State Location†

R. Bisson, M. Sacchi, T. T. Dang, B. Yoder, P. Maroni, and R. D. Beck*

Laboratoire de Chimie Physique Moléculaire, Ecole Polytechnique Fédérale de Lausanne, CH-1015 Lausanne, Switzerland

Received: July 31, 2007; In Final Form: October 5, 2007

Quantum state-resolved sticking coefficients on Pt(111) and Ni(111) surfaces have been measured for CH_4 excited to the first overtone of the antisymmetric C−H stretch ($2\nu_3$) at well-defined kinetic energies in the range of 10−90 kJ/mol. The ground-state reactivity of CH_4 is approximately 3 orders of magnitude lower on Ni(111) than on Pt(111) for kinetic energies in the range of 10−64 kJ/mol, reflecting a difference in barrier height of 28 ± 6 kJ/mol. $2\nu_3$ excitation of CH_4 increases its reactivity by more than 4 orders of magnitude on Ni(111), whereas on Pt(111) the reactivity increase is lower by 2 orders of magnitude. We discuss the observed differences in the state-resolved reactivity for the ground state and $2\nu_3$ excited state of methane in terms of a difference in barrier height and transition state location for the dissociation reaction on the two metal surfaces.

Introduction

State-resolved reactivity measurements are fundamental to the understanding of chemical reaction dynamics for both gas phase and gas/surface reactions. The investigation of the latter reaction type has seen significant progress over the past few years due to the combination of laser excitation in molecular beams and UHV surface analysis techniques. Since the initial report of a state-specific reactivity measurement by Juurlink et al.,[1] several groups have succeeded in performing such detailed measurements.[2−5] To date, most state-resolved reactivity studies concern the chemisorption of methane on the Ni(100) and Ni(111), motivated by the fact that these surfaces are models for nickel catalysts used in steam reforming.[6] The steam reforming process, which converts natural gas into H_2 and CO, is of tremendous economical importance because it is the dominant method for large-scale production of hydrogen as well as the starting point for many synthetic processes in the chemical industry.

Another important and widely studied model catalytic surface is Pt(111), which has attracted interest due to its relatively simple preparation in UHV and the high selectivity of platinum catalysts for the generation of reforming products.[7] Luntz and Bethune[8] have used molecular beam techniques to probe the effect of translational energy on the sticking probability of CH_4 on Pt(111) and found a near-exponential increase in reactivity with increasing normal kinetic energy. As in the case of nickel, this normal energy scaling of the reactivity suggests a direct reaction mechanism with a substantial barrier. Luntz and Bethune also investigated the effect of vibrational energy of the incident CH_4 on its reactivity on the Pt(111) surface. Using two different carrier gases (H_2 and He) and nozzle temperatures (300 and 680 K), they prepared CH_4 in molecular beams with identical kinetic energy but different vibrational energy content. They observed a 2-fold higher reactivity for the hot CH_4/He mixture as compared to the cooler CH_4/H_2 mixture. While their experiments probed the effect of vibrational excitation averaged over all vibrational modes of CH_4, Luntz and Bethune pointed out that they have "no way of determining the relative effectiveness of added energy in different vibrational modes for promoting the dissociation," which is the main motivation for performing state-resolved reactivity measurements.

The only state-resolved reactivity measurement for methane on Pt(111) has been reported by Higgins et al.[2] The authors used cw-laser excitation in a build-up cavity to excite methane to the $2\nu_3$ antisymmetric C−H stretch vibration and probed the reaction products by thermal helium scattering. They reported a 30-fold reactivity enhancement upon excitation of the $2\nu_3$ state at incident normal kinetic energy of 5.4 kJ/mol, much lower than the more than 4 orders of magnitude enhancement observed for the same quantum state of CH_4 on Ni(100).[3] Comparison of the effect of vibrational and translational energy on the CH_4 dissociation probability on Pt(111) shows that adding 72 kJ/mol of vibrational energy via $2\nu_3$ excitation produces the same increase in reactivity as 30 kJ/mol of normal translational energy. This pronounced difference in the effect of translational and vibrational energy provides evidence for a non-statistical reaction mechanism, which does not simply scale with total available energy as it is assumed in the PC-MURT model of Harrison.[9]

In the present study, we employ a different method for reactant excitation and product detection than Higgins et al., while extending the state-resolved reactivity measurements for the $2\nu_3$ state of CH_4 on Pt(111) to a range of incident kinetic energies from 10 to 64 kJ/mol. Furthermore, we report state-resolved $2\nu_3$ reactivity data and laser-off data for CH_4 on Ni(111) over a similar range of incident kinetic energy. Comparison of the state-resolved reactivity for the ground state and $2\nu_3$ excited state of CH_4 on Pt(111) and Ni(111) yields information about the difference in barrier height and location for methane dissociation on the two surfaces.

Experimental Section

Our state-resolved sticking coefficient measurements are performed in a molecular beam/surface science apparatus

† Part of the "Giacinto Scoles Festschrift".

* Corresponding author. E-mail: rainer.beck@epfl.ch.

10.1021/jp076082w CCC: $37.00
Published on Web 11/14/2007

designed to study the surface interactions of laser-excited molecules. Since the apparatus has been described previously in detail,[10] we only summarize the most important features here. The experimental setup consists of a triply differentially pumped molecular beam source connected to an ultrahigh vacuum surface science chamber (base pressure 6×10^{-11} mbar). We generate a pulsed molecular beam by expanding mixtures of methane (99.9995% purity) and hydrogen (99.9999% purity) through a temperature-controlled solenoid valve with an open time of 300 μs. The beam pulses pass through a 1 mm diameter skimmer into the second differential pumping region where their duration is reduced to 30 μs by a chopper wheel rotating at 200 Hz. After a further differential pumping stage, the beam pulses enter the UHV chamber through a 1 mm diameter aperture, traverse a laser beam alignment tool, and impinge on a single-crystal surface at normal incidence. The alignment tool serves to overlap the molecular beam with the laser beam, which is focused to a line by a cylindrical lens and crosses the molecular beam at 90°. The length of the line focus and the duration of the gas pulses are matched so that, depending on the speed of the beam, between 33% and 100% of the methane molecules are exposed to the excitation laser.

We produce infrared laser pulses, tunable in the vicinity of 1.7 μm (6000 cm^{-1}), by generating the difference frequency between the fundamental output of an injection seeded single mode Nd:YAG laser and a narrow band dye laser in a lithium niobate crystal. We amplify the resulting 1−2 mJ pulses of tunable IR to 140 mJ/pulse in a two-stage optical parametric amplifier using two KTP crystals. To ensure that the infrared laser is tuned into resonance with the selected ro-vibrational transition of methane during deposition, we split off a small portion of the IR beam and monitor the cavity ring-down signal in a separate expansion chamber. We also use the cavity ring-down spectra of CH_4 in the jet expansion to obtain rotational level population information needed for the sticking coefficient determination. Taking into account the measured population in $v = 0$, $J = 1$ and the speed-dependent overlap of the molecular beam with the IR laser focus, the fraction of excited molecules in the molecular beam varies from 9% to 18% depending on the CH_4/carrier gas mixture used.

The molecular beam pulses impinge at normal incidence on the 10 mm diameter single-crystal surface (Pt(111) or Ni(111)) oriented to within 0.1°. The surface is cleaned in the UHV chamber by Ar^+ sputtering/annealing cycles until impurities can no longer be detected by Auger electron spectroscopy (AES). We measure the translational energy, E_t, of the methane molecules in the beam by time-of-flight using the chopper wheel and an on-axis quadrupole mass spectrometer. We adjust E_t from 10 kJ/mol to 55 kJ/mol by varying the seed ratio of CH_4 in H_2 from 100% to 1% at a constant nozzle temperature of 323 K. Increasing the nozzle temperature to $T_n = 373$ K for the 1% CH_4 in H_2 mixture allows us to reach a translational energy of 64 kJ/mol. To determine absolute sticking coefficients for methane, we perform a timed exposure of the clean crystal surface to the molecular beam, measuring both the incident dose of CH_4 molecules per unit area as well as the resulting surface density of carbon reaction products on the surface. Initial sticking coefficients S_0 are calculated as the ratio between the surface density of carbon and the incident dose per unit area in the limit of low coverage (5−10% ML). We determine the incident flux of methane [molecules s^{-1} cm^{-2}] onto the surface from the methane partial pressure rise due to the molecular beam monitored by a calibrated quadrupole mass spectrometer together with the beam cross section at the surface, which is measured by AES to be 0.03 cm^2. The primary reaction products of the direct methane chemisorption on Pt(111) and Ni(111) are adsorbed methyl and hydrogen according to[11]

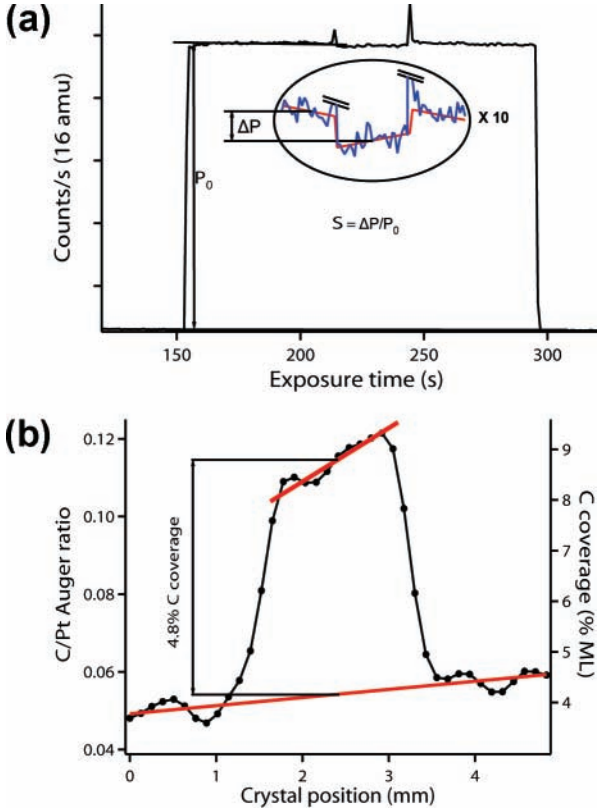

Figure 1. (a) Example of a King & Wells measurement of the CH_4 sticking coefficient on Pt(111) averaged over a 30 s deposition. Repeated measurements give an averaged sticking coefficient $S = (0.98 \pm 0.16) \times 10^{-2}$, which is used to calibrate the reactivity measurement via Auger detection of adsorbed carbon. (b) AES analysis of carbon coverage resulting from a 30 s exposure under conditions identical to those in Figure 1a. The C/Pt AES ratio is calculated from C(272 eV) and Pt(237 eV) Auger signals. The change in the C/Pt AES ratio is related to a change in carbon coverage (in %ML), using the averaged K&W sticking coefficient and the calibrated exposure flux.

$$CH_4(g) \rightarrow CH_3(ads) + H(ads) \qquad (1)$$

We perform depositions at a surface temperature of 600 K for Pt(111) and 475 K for Ni(111), temperatures at which the methyl radicals quickly dehydrogenate and the hydrogen leaves the surface by recombinative desorption of H_2.[12] The carbon atoms remain on the metal surface and are detected by AES. Once a deposition is complete, we quantify the C coverage, recording C and Pt (or Ni) AES signals at typically 80 positions across the surface in a computer controlled scan.

For the reactivity measurements on the Pt(111) surface, we calibrate the C/Pt AES signal ratio in terms of C coverage by comparison to King & Wells (K&W) measurements[13] rather than using a carbon uptake curve to a known saturation coverage as done for the Ni(111) surface.[10] The reason for using a different calibration procedure stems from the fact that C on Pt(111) can adsorb either in a carbidic or in a graphitic phase with different saturation coverages.[9] The K&W method is a self-calibrating technique for sticking coefficient measurements, which uses a mass spectrometer to compare the reflectivity for the incident methane molecules on an inert surface (i.e., mica) to that of the clean reactive surface (Figure 1a). The limited sensitivity of the K&W method allows for sticking coefficient

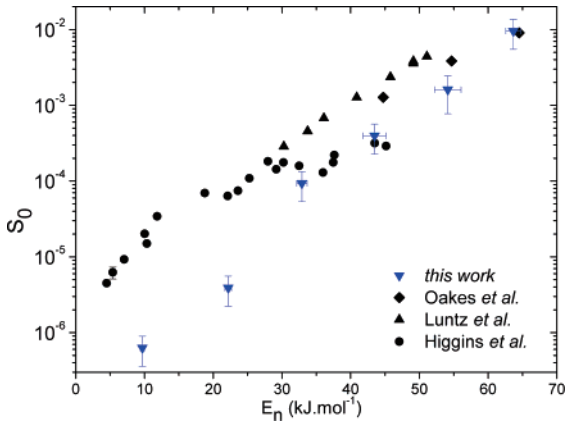

Figure 2. Laser-off reactivity of CH_4 on Pt(111) as a function of normal kinetic energy (E_n): (▼) this work, $T_s = 600$ K, $T_n = 323-373$ K; (▲) Luntz et al., $T_s = 800$ K, $T_n = 300$ K; (◆) Oakes et al., $T_s = 550$ K, $T_n = 500-1000$ K; (●) Higgins et al., $T_s = 575$ K, $T_n = 295-1073$ K.

measurements above 5×10^{-3} in our setup. We therefore use a CH_4 beam at high kinetic energy (64 kJ/mol) and high nozzle temperature (473 K) to perform the Auger calibration. Under these conditions, we measure the sticking coefficient of CH_4 on a clean Pt(111) surface averaged over a 30 s deposition to be $S = (0.98 \pm 0.16) \times 10^{-2}$ with the error obtained by repeated measurements (95% confidence). The relative error of 16% is taken into account in all reactivity measurements using the calibrated C/Pt AES signals. Auger analysis of the carbon "spot" resulting from the same CH_4 molecular beam dose of the clean Pt(111) surface yields a C(272 eV)/Pt(237 eV) AES signal ratio of 0.062 (Figure 1b). During the exposure, the incident CH_4 dose was monitored by a calibrated mass spectrometer to be 4.9 ML in terms of Pt atom surface density (1.50×10^{15} cm^{-2} on Pt(111)). We use the sticking coefficient from the K&W measurement along with the measured flux to calibrate the C/Pt AES signal ratio in terms of carbon coverage, that is, $0.98 \times 10^{-2} \times 4.9$ ML $= 0.048$ ML for a C/Pt AES signal ratio of 0.062. Once calibrated, we use AES detection of C on Pt(111) to quantify the sticking coefficient in the range of incident energy of 10−64 kJ/mol with a lower nozzle temperature (323 and
373 K) for both laser-off and $2\nu_3$ state reactivity. Even though the calculated $2\nu_3$ state-resolved sticking coefficients are well above the detection limit of the K&W technique, the low fraction of laser excited CH_4 in the molecular beam prevents the use of the K&W method for calibration of the laser-on sticking coefficients because our laser-on measurements probe the average sticking coefficient of all CH_4 molecules contained in the beam (excited and unexcited).

We calculate the initial sticking coefficients S_0 from the measured C/Pt AES signal ratios of typically 0.05−0.1 (corresponding to 4−8% ML coverage) detected at the end of a deposition experiment. In the calculation of S_0, we correct for the nonlinearity in carbon uptake using the experimentally determined uptake curve for carbon on Pt(111), produced by methane molecular beam exposure.

Results and Discussion

Figure 2 shows the laser-off reactivity for CH_4 on Pt(111) as a function of kinetic energy for normal incidence and a surface temperature of 600 K. At the moderate nozzle temperatures used (323−373 K), the data represent a close upper limit to the ground-state sticking coefficient $S_0(v = 0)$. We observe a near exponential increase in reactivity by 4 orders of magnitude, when the incident kinetic energy is raised from 10 to 64 kJ/mol.

For comparison, we have included in Figure 2 the results of several previous studies of CH_4 sticking coefficients on Pt(111).[2,8,14] One observes significant deviations between the data sets reported by different groups. Some of the differences can be attributed to different surface and/or nozzle temperatures used in the various studies. The data reported by Luntz et al. were recorded at a surface temperature of 800 K, whereas our experiments used $T_s = 600$ K. If we take into account the experimentally observed surface temperature dependence of the methane sticking coefficient reported by Luntz et al., our results are in reasonable agreement. Taking into account the difference in T_n and T_s, the data reported by Oakes et al. also agree with our data at high kinetic energy.

On the other hand, the data reported by Higgins et al.[2] were recorded at similar surface temperature (575 vs 600 K) but show a significantly higher reactivity and smaller slope with increasing kinetic energy than our results. Higgins et al. varied the nozzle temperature from 295 to 1073 K to increase the normal kinetic energy of the CH_4 in He beam from 5 to 44 kJ/mol and of the CH_4 in H_2 beam from 22 to 52 kJ/mol. Raising the nozzle temperature will increase both the kinetic energy and the average vibrational energy of the methane molecules. One would expect the simultaneous increase of kinetic and vibrational energy to produce a steeper slope than that observed in our data where only the kinetic energy was changed, because the reactivity of methane on Pt(111) is known to increase with increasing average vibrational energy.[8] However, an opposite trend is observed between the data of Higgins et al. and our data. Furthermore, below $E_n = 30$ kJ/mol, there is more than an order of magnitude difference between our results and those of Higgins et al. In their measurements, Higgins et al. used a continuous molecular beam, whereas we employed a pulsed molecular beam with higher instantaneous gas flux. To exclude the possibility that this higher instantaneous flux of CH_4 in H_2 could lead to a transient passivation of the Pt(111) surface by the adsorption of hydrogen, we repeated a number of laser-off reactivity measurements with a continuous beam produced by a pinhole nozzle of 30 μm diameter with no detectable difference in the results. We also compared the reactivity of a pulsed beam of 25% CH_4 in H_2 to that of a beam of 3% CH_4 in He at identical nozzle temperature and very similar kinetic energies and detected no significant difference in reactivity. Finally, our reactivity measurement at $E_n = 10$ kJ/mol is obtained with a pure beam of CH_4, which excludes hydrogen passivation from the carrier gas but which shows no deviation from the trend of lower sticking coefficients as compared to those observed by Higgins et al. We can therefore only speculate reasons for the discrepancy between our results and those of Higgins et al. The high sensitivity of the TEAS method used by Higgins et al. and the fact that the sticking coefficients were measured for very low coverages (<1% ML) could cause their measurements to be influenced by surface defects. The reactivity at step edges and kink sites, which are present on a single-crystal surface in concentrations depending on the miscut, sample preparation, and history, is known to be significantly higher than that on terraces,[15] which could lead to a higher (averaged) sticking coefficient measured at low incident energy where the reactivity on the terraces is still exceedingly low.

Figure 3 shows the state-resolved sticking coefficients for CH_4 excited to $2\nu_3$, the first overtone of the antisymmetric stretch vibration, via the R(1) ro-vibrational transition. The

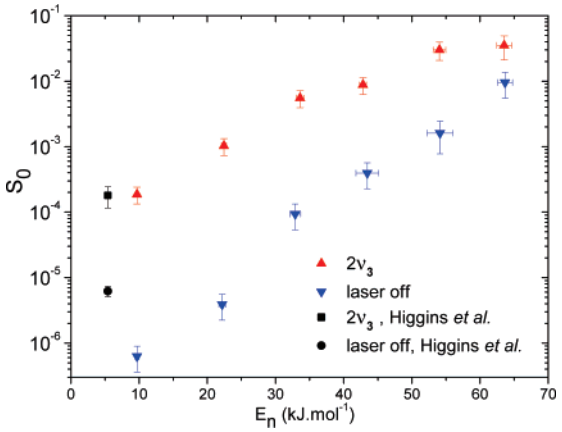

Figure 3. Sticking coefficients as a function of incident kinetic energy (normal incidence) for dissociative chemisorption of CH_4 on Pt(111). (▼) Laser-off data giving an upper limit for $S_0(v = 0)$, (▲) state-resolved sticking coefficients for $2\nu_3$, $J = 2$. Error bars are 95% confidence of convoluted uncertainties. For comparison, we also show the data obtained by Higgins et al., (■) $2\nu_3$, $J = 1,2$, (●) laser-off.

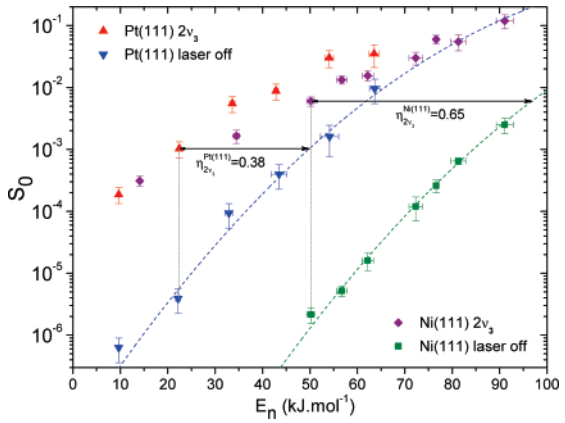

Figure 4. Comparison of the $2\nu_3$ and laser-off reactivity for Pt(111) ($T_s = 600$ K) and Ni(111) ($T_s = 475$ K): (▲)$2\nu_3$, Pt(111); (▼) laser-off, Pt(111); (◆) $2\nu_3$, Ni(111); (■) laser-off, Ni(111). Dashed lines are "S"-shaped curves, fitted to the laser-off data and used to determine the difference in average barrier height ΔE_a between Pt(111) and Ni-(111). The vibrational efficacies $\eta_{2\nu_3}$ for Pt(111) and Ni(111) are calculated at the incident kinetic energies indicated by the vertical dotted lines. The horizontal arrows indicate the amount of normal kinetic energy, which produces the same increase in reactivity as the excitation into the $2\nu_3$ vibrational state.

normal mode label $2\nu_3$ for the vibrationally excited eigenstate prepared by our narrowband laser is only an approximation. For CH_4, the fundamental frequencies of the two stretch modes are approximately twice those of the two bending modes, leading to stretch−bend coupling between the normal mode vibrations (Fermi resonances). The resulting eigenstates in the presence of the anharmonic coupling can be described as a superposition of the four normal mode fundamentals ν_i, $i = 1-4$. Wang et al.[16] used Van Vleck perturbation theory and an ab initio force field to calculate the vibrational states of CH_4 up to 9000 cm^{-1} and gave the leading coefficients in a normal mode expansion. According to their calculations, the state prepared in this work is composed of 79% $2\nu_3$ character and 15% $\nu_1+\nu_3$, where ν_1 and ν_3 are the symmetric and antisymmetric C−H stretch fundamentals, respectively.

At $E_t = 10$ kJ/mol, the lowest incident energy investigated by us, we observe a 300-fold increase in reactivity upon $2\nu_3$ excitation. Higgins et al. reported a factor of 30 increase at the same total kinetic energy but for an incidence angle of 45°, corresponding to a normal energy of 5.4 kJ/mol, primarily because their laser-off measurement of S_0 is higher (Figure 3). Because T_s (575 and 600 K) and T_n (298 and 323 K) for the two measurements are nearly identical, we can again only speculate that their laser-off measurement reflects at least in part the reactivity at step edges or other defects and that the reaction at these sites is less strongly activated by $2\nu_3$ excitation.

Figure 4 shows a comparison of our state-resolved sticking coefficient measurements (laser-off and for $2\nu_3$) on Pt(111) and Ni(111). A couple of differences between the data sets for the two metals are readily apparent. The laser-off reactivity on Ni-(111) is approximately 3 orders of magnitude lower than that on Pt(111), and we detect a much stronger enhancement in reactivity upon $2\nu_3$ excitation for Ni(111).

The lower laser-off reactivity for Ni(111) at a given incident kinetic energy is consistent with a higher barrier for methane dissociation on Ni(111) as compared to Pt(111). Although barrier heights reported in the literature vary over a considerable range, comparative studies treating both metal surfaces at the same level of theory found a higher barrier for Ni(111) than for Pt-(111).[17,18] We use our laser-off results for Pt(111) and Ni(111) to estimate the difference in barrier height on the two surfaces. Because our two data sets were recorded at different surface temperatures (600 K for Pt(111) and 475 K for Ni(111) to facilitate comparison with previous studies[19−21]), we correct the laser-off data for Pt(111) using the experimentally determined surface temperature dependence of S_0 by Luntz et al.[8] We then use "S"-shaped curves, initially proposed by Luntz,[22] to parametrize the variation of the laser-off sticking coefficients with kinetic energy E_n:

$$S_0(E_n) = \frac{A}{2}\left[1 + erf\left(\frac{E_n - E_0}{W}\right)\right] \qquad (2)$$

where E_0 is the average barrier height, W is the width of a Gaussian distribution of barrier heights, and A is the asymptotic value of S_0 at high E_n.

We fix $A = 1$ and determine E_0 and W as fitting parameters by least-squares fits of eq 2 to the laser-off data for Pt(111) and Ni(111). These fits yield similar values for W on both metals ($W_{CH_4/Pt(111)} \approx W_{CH_4/Ni(111)} \approx 31 \pm 2$ kJ/mol), reflected in the parallel rise of the "S"-shaped curves in Figure 4. When compared to that of Pt(111), the fit for Ni(111) gives a higher average barrier height of $\Delta E_a = 28 \pm 6$ kJ/mol. Such a difference in barrier height is in good agreement with the comparative theoretical studies by Lia et al.[18] and Anderson et al.,[17] which found a higher reaction barrier on Ni(111) than on Pt(111) by 31 and 21 kJ/mol, respectively.

In addition to the much lower ground-state methane reactivity on Ni(111) as compared to Pt(111), we also observe a much greater reactivity increase on Ni(111) than on Pt(111) upon $2\nu_3$ excitation. While at first glance, one might consider this to be a consequence of the difference in barrier height for the two metals, we suggest that the different degree of reactivity enhancement is related to different transition state geometries on the two surfaces. Considering only a difference in barrier height, it is difficult to rationalize that at the low reaction probability of $S_0 \approx 3 \times 10^{-6}$ where the reaction is still "starved for energy" on both surfaces, the addition of 72 kJ/mol of $2\nu_3$ vibrational energy increases the reactivity to only 1×10^{-3} for the lower barrier system CH_4/Pt(111), while for the higher barrier system CH_4/Ni(111) the reactivity increases all the way to 1×10^{-2}.

This difference in the degree of vibrational activation between Ni(111) and Pt(111) is also reflected in their different vibrational efficacies $\eta_{2\nu_3}$, which compare the effect of translational and

$2\nu_3$ vibrational energy on the reactivity on each surface. $\eta_{2\nu_3}$ is defined as:

$$\eta_{2\nu_3} = \frac{\Delta E_n}{\Delta E_{2\nu_3}} \quad (3)$$

where ΔE_n is the amount of normal energy required to achieve the same increase in reactivity as observed for the addition of $\Delta E_{2\nu_3} = 72$ kJ/mol of vibrational energy by excitation of the $2\nu_3$ state.

In Figure 4, we have indicated the $2\nu_3$ efficacies for the two surfaces, calculated at incident energies where we measure similar laser-off reactivities, on the order of 3×10^{-6} for both surfaces. The stronger effect of $2\nu_3$ excitation on Ni(111) is reflected by a higher efficacy $\eta_{2\nu_3}^{Ni(111)} = 0.65$, nearly twice the value for Pt(111) $\eta_{2\nu_3}^{Pt(111)} = 0.38$. Such an increased vibrational efficacy is typically associated with a "late" barrier on a simple Polanyi-type model potential energy surface[23] and corresponds to a transition state structure for which the dissociating bond is significantly stretched at the transition state. Calculated transition state geometries are consistent with this interpretation and predict the methane molecule on the top site above a surface metal atom for both Pt(111) and Ni(111), but with the reactive C−H bond more elongated on Ni(111)[17,24−26] than on Pt-(111).[17,27] The proposed difference in barrier location (later on Ni(111) than on Pt(111)) is also consistent with previous results reported by Luntz and Bethune,[8] who reported an averaged vibrational efficiency $\beta_v = d(\ln S_0)/d(\langle E_v \rangle)$ of all thermally populated states in a hot nozzle beam to be 4 times higher for Ni(111) than for Pt(111).

Summary and Conclusion

In summary, we report state-resolved measurements of the reactivity of CH_4 in the $2\nu_3$ and ground state on Pt(111) and Ni(111). We observe much lower ground-state reactivity on Ni-(111) combined with higher reactivity enhancement upon $2\nu_3$ excitation than for Pt(111). Comparison of the ground-state reactivity data suggests the average barrier height on Ni(111) exceeds that of Pt(111) by $\Delta E_a = 28 \pm 6$ kJ/mol. The higher $2\nu_3$ efficacy for the dissociation of CH_4 on Ni(111) as compared to Pt(111) suggests a transition state structure with a larger bond length for the dissociating C−H bond on Ni(111), consistent with previous theoretical results.

Acknowledgment. Financial support by the Swiss National Science Foundation through grant 200020-115972/1 and the EPFL is gratefully acknowledged.

References and Notes

(1) Juurlink, L. B. F.; McCabe, P. R.; Smith, R. R.; DiCologero, C. L.; Utz, A. L. *Phys. Rev. Lett.* **1999**, *83*, 868.
(2) Higgins, J.; Conjusteau, A.; Scoles, G.; Bernasek, S. L. *J. Chem. Phys.* **2001**, *114*, 5277.
(3) Schmid, M. P.; Maroni, P.; Beck, R. D.; Rizzo, T. R. *J. Chem. Phys.* **2002**, *117*, 8603.
(4) Beck, R. D.; Maroni, P.; Papageorgopoulos, D. C.; Dang, T. T.; Schmid, M. P.; Rizzo, T. R. *Science* **2003**, *302*, 98.
(5) Maroni, P.; Papageorgopoulos, D. C.; Sacchi, M.; Dang, T. T.; Beck, R. D.; Rizzo, T. R. *Phys. Rev. Lett.* **2005**, *94*, 246104.
(6) Spath, P. L.; Mann, M. K. National Renewable Energy Laboratory Technical Report, NREL/TP-570-27637, 2001.
(7) Zaera, F. *Appl. Catal., A* **2002**, *229*, 75.
(8) Luntz, A. C.; Bethune, D. S. *J. Chem. Phys.* **1989**, *90*, 1274.
(9) DeWitt, K. M.; Valadez, L.; Abbott, H. L.; Kolasinski, K. W.; Harrison, I. *J. Phys. Chem. B* **2006**, *110*, 6705.
(10) Schmid, M. P.; Maroni, P.; Beck, R. D.; Rizzo, T. R. *Rev. Sci. Instrum.* **2003**, *74*, 4110.
(11) Lee, M. B.; Yang, Q. Y.; Tang, S. L.; Ceyer, S. T. *J. Chem. Phys.* **1896**, *85*, 1693.
(12) Koel, B. E.; White, J. M.; Goodman, D. W. *Chem. Phys. Lett.* **1982**, *88*, 236.
(13) King, D. A.; Wells, M. G. *Surf. Sci.* **1972**, *29*, 454.
(14) Oakes, D. J.; McCoustra, M. R. S.; Chesters, M. A. *Faraday Discuss.* **1993**, 325.
(15) Egeberg, R. C.; Ullmann, S.; Alstrup, I.; Mullins, C. B.; Chorkendoff, I. *Surf. Sci.* **2002**, *497*, 183.
(16) Wang, X. G.; Sibert, E. L. *J. Chem. Phys.* **1999**, *111*, 4510.
(17) Anderson, A. B.; Maloney, J. J. *J. Phys. Chem.* **1988**, *92*, 809.
(18) Liao, M. S.; Au, C. T.; Ng, C. F. *Chem. Phys. Lett.* **1997**, *272*, 445.
(19) Juurlink, L. B. F.; Smith, R. R.; Killelea, D. R.; Utz, A. L. *Phys. Rev. Lett.* **2005**, *94*.
(20) Lee, M. B.; Yang, Q. Y.; Ceyer, S. T. *J. Chem. Phys.* **1987**, *87*, 2724.
(21) Smith, R. R.; Killelea, D. R.; DelSesto, D. F.; Utz, A. L. *Science* **2004**, *304*, 992.
(22) Luntz, A. C. *J. Chem. Phys.* **2000**, *113*, 6901.
(23) Polanyi, J. C. *Acc. Chem. Res.* **1972**, *5*, 161.
(24) Burghgraef, H.; Jansen, A. P. J.; Vansanten, R. A. *J. Chem. Phys.* **1994**, *101*, 11012.
(25) Kratzer, P.; Hammer, B.; Norskov, J. K. *J. Chem. Phys.* **1996**, *105*, 5595.
(26) Yang, H.; Whitten, J. L. *J. Chem. Phys.* **1992**, *96*, 5529.
(27) Psofogiannakis, G.; St-Amant, A.; Ternan, M. *J. Phys. Chem. B* **2006**, *110*, 24593.